NUWC-NPT Technical Report 11,298
1 August 2001

An Examination of Wake Oscillator Models for Vortex-Induced Vibrations

Leslie Ng
Richard H. Rand
Cornell University

Timothy Wei
Rutgers University

William L. Keith
NUWC Division Newport

Naval Undersea Warfare Center Division
Newport, Rhode Island

TABLE OF CONTENTS

LIST OF ILLUSTRATIONS

AN EXAMINATION OF WAKE OSCILLATOR MODELS FOR VORTEX-INDUCED VIBRATIONS

INTRODUCTION

Experimental results for vortex-induced vibrations of both pivoted and non-pivoted cylinders in a crossflow are presented in this report. Simplified models involving two ordinary differential equations are reviewed and shown to exhibit many of the features of the experimental results. Results of perturbation analysis of the simplified models are presented and used to explain some qualitative features, such as resonant frequency locking and hysteresis, in terms of bifurcations in the slow flow.

In an experiment by Wei,[1] a cylinder attached to a leaf spring is placed at the bottom of a flow tank (figure 1a). Since the leaf spring restricts the motion of the cylinder, the end attached to the spring remains fixed, and the cylinder can only pivot around that point at an angle transverse to the oncoming flowing water. Since the leaf spring also provides a restoring force, the cylinder tends to stay in the upright position if there are no external forces applied. As water flows past the cylinder, vortices are shed along the length of the cylinder on alternating sides, providing a periodic force on the cylinder.

Figure 2 depicts data from the experiment by Wei. Note that for a range of flow speeds, the frequency of vortex shedding is the same as the cylinder oscillation frequency. This effect, called resonance lock-in, involves large-amplitude periodic motions of the cylinder near its natural frequency. Outside of this resonance region, the vortex-shedding frequency varies linearly with the flow velocity via the Strouhal relation:

$$f_n = \frac{SV}{D}, \tag{1}$$

where S is the Strouhal number, V is the flow velocity, and D is the diameter of the cylinder.

The features observed in Wei's pivoted cylinder experiment are similar to features observed in experiments where the entire cylinder is allowed to move transversely to the flow; figures 1a and 1b illustrate the pivoted and non-pivoted cylinder systems, respectively. Figure 3 shows the experimental results from a study by Feng[2] of a non-pivoted cylinder in a crossflow of air.

The data in figures 2 and 3 share many common features. Although the details of the fluid flow (including, for example, the coherent vortices) are expected to be different for these two types of experiments, the phenomenon of resonance lock-in is common to both. One feature present in the data in figure 2 that is not present in the figure 3 data is a part of the lock-in region where the frequency varies linearly with flow speed (labeled *II* and $S = 0.18$). This is because Wei's study uses water as the fluid, and Feng's study uses air as the fluid. The difference

between these two experiments can be quantified by using the ratio of cylinder mass to the mass of the displaced fluid, which is an important quantity in the behavior of vortex-induced vibration experiments. This mass ratio is low for Wei's study using water and high for Feng's study using air. For more on the role of the mass ratio, see Govardhan and Williamson[3] and Khalak and Williamson.[4] For an overview of vortex-induced vibrations, see Blevins.[5]

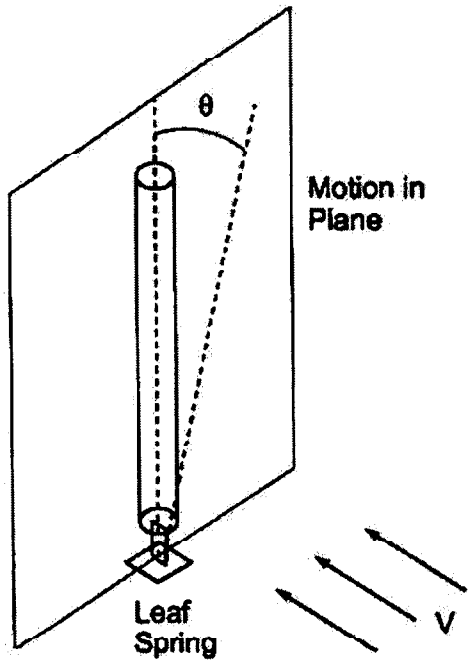

Figure 1a. Setup for Pivoted Cylinder Experiments

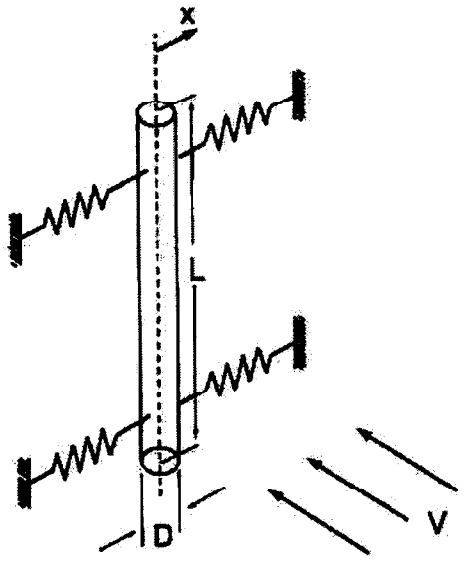

Figure 1b. Setup for Non-Pivoted Cylinder Experiments

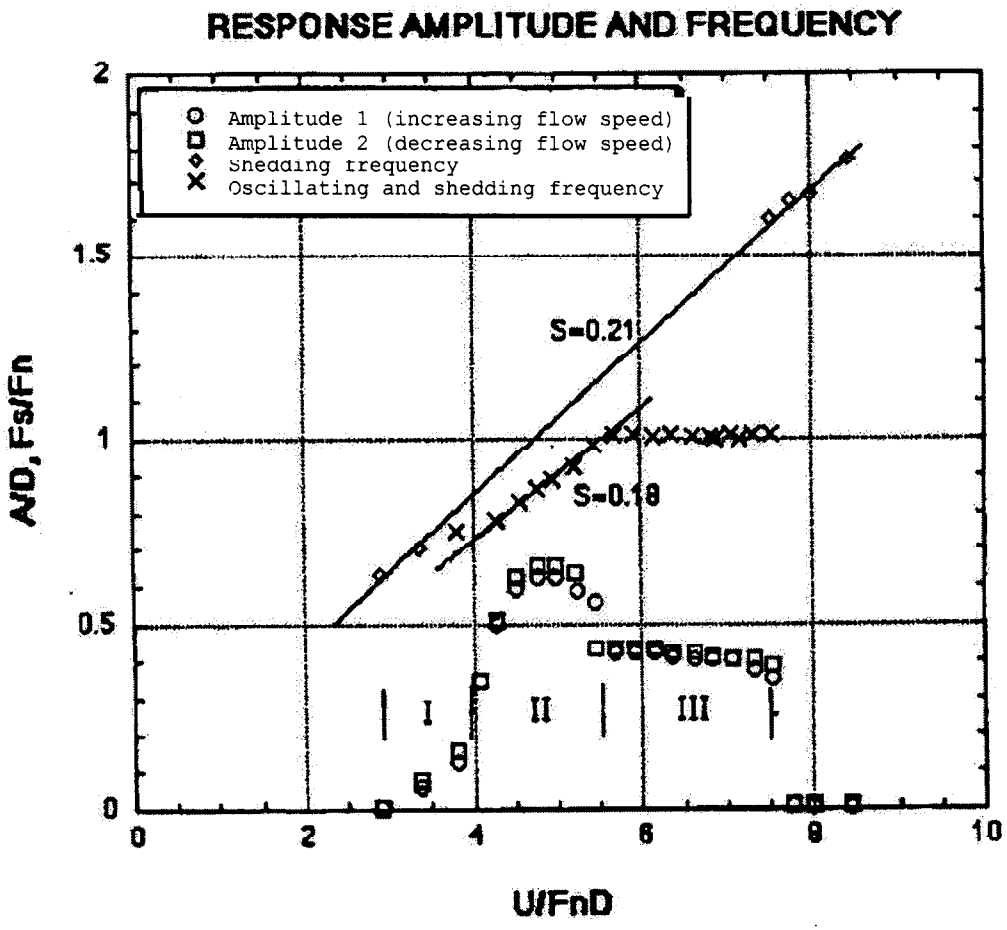

Figure 2. Experimental Data for a Pivoted Cylinder in Water (Data from Wei[1]). (Note that both the amplitude of cylinder oscillation (lower portion of plot) and frequency (upper portion of plot) are displayed as functions of flow speed.)

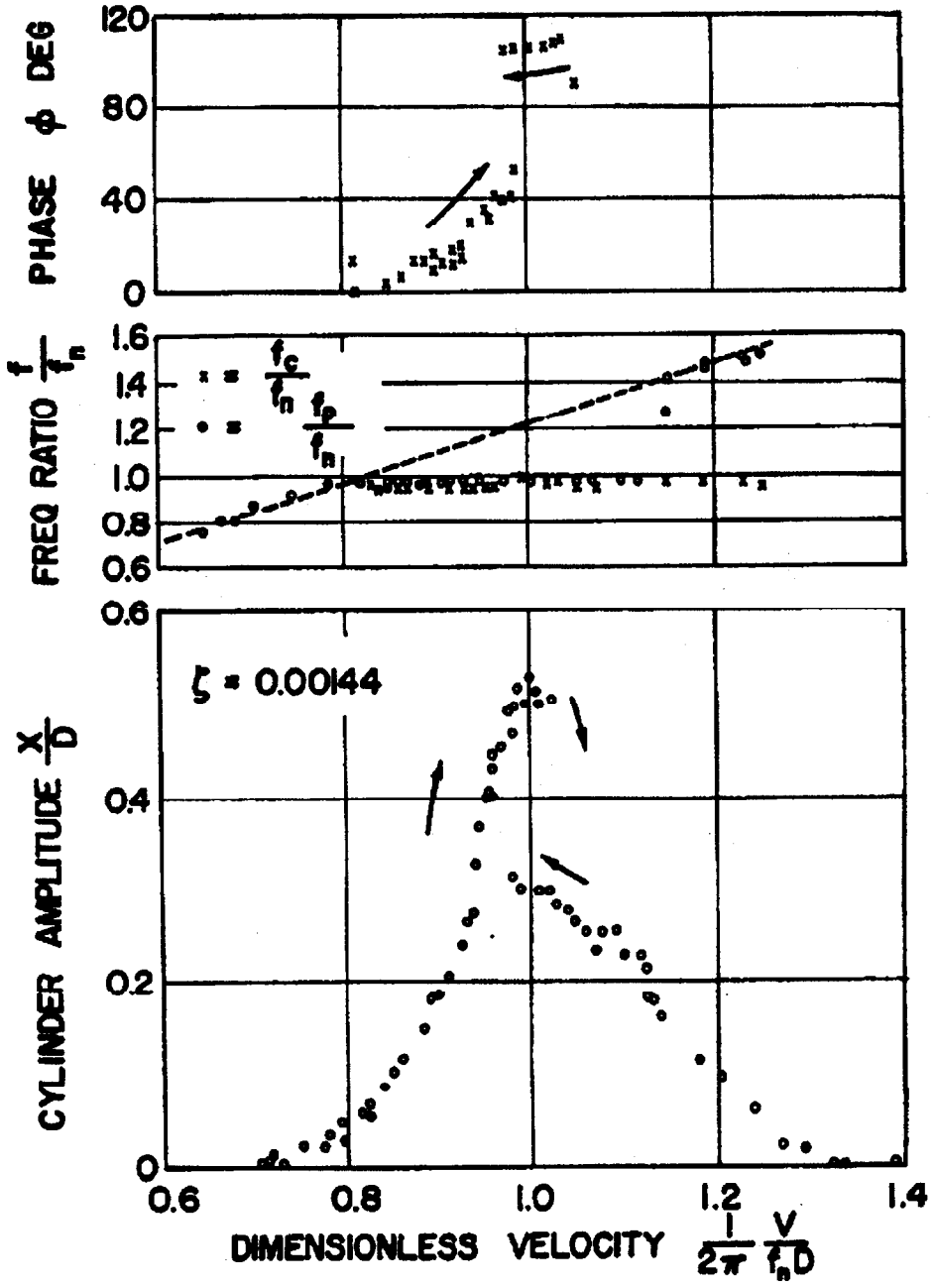

Figure 3. Experimental Data for a Non-Pivoted Cylinder in an Air Flow (taken from Hartlen and Currie[8])

In the following section, a model will be analyzed that was originally derived to explain resonance lock-in in the non-pivoted experiment shown in figure 1b. However, since pivoted (figure 1a) and non-pivoted (figure 1b) experiments each exhibit resonance lock-in, the model may be used to explain some features of Wei's data (figure 2).

ANALYSIS OF WAKE OSCILLATOR MODELS

Semi-empirical models for vortex-induced vibrations of cylinders have been widely studied. A review article by Parkinson[6] presents a good summary of these models. A van der Pol-type oscillator is commonly used to represent the time varying forces on the cylinder due to vortex shedding. The idea was first suggested by Bishop and Hassan.[7] These types of models are known as wake oscillator models. Hartlen and Currie[8] first proposed the following model in non-dimensionalized form:

$$\ddot{x} + 2\zeta\dot{x} + x = a\,\omega^2 y\,, \tag{2}$$

$$\ddot{y} + \omega^2 y - \alpha\,\omega\,\dot{y} + \frac{\gamma}{\omega}\dot{y}^3 = b\dot{x}\,, \tag{3}$$

where x is the dimensionless cylinder displacement and y is a representative fluid property, for example, pressure or lift coefficient. The dots represent differentiation with respect to time t, and ω is proportional to the flow speed of the system, of which α, ζ, γ, a, and b are parameters. Here the cylinder and its elastic restraint are modeled by a damped linear oscillator (equation (2)), and the periodic vortex shedding of the fluid is modeled by a limit cycle oscillator (equation (3)). These two ordinary differential equations are assumed to be linearly coupled. Note that the fluid drag force on the rod $\dot{x}|\dot{x}|$ has been omitted.

Figure 4 shows the results of numerically integrating equations (2) and (3) using the original parameter values (equation (4)) in the study by Hartlen and Currie. These parameter values correspond to the experimental setup in figure 1b for the data in figure 3:

$$\zeta = 0.0015,\ \alpha = 0.02,\ \gamma = \frac{2}{3},\ a = 0.002,\ \text{and}\ b = 0.4\,. \tag{4}$$

Figure 4 was obtained by numerically integrating equations (2) and (3) for a long time interval until most of the transients expired and the remaining steady-state motion was periodic. Comparing figure 4 with figures 2 and 3, it can be seen that some of the features observed in these experiments are reproduced by the Hartlen-Currie model. A large cylinder-oscillation amplitude resonance region occurs when the vortex-shedding frequency is near the natural frequency of the cylinder. Also, the frequency of oscillation in this region is nearly constant at a value close to the natural frequency of the cylinder.

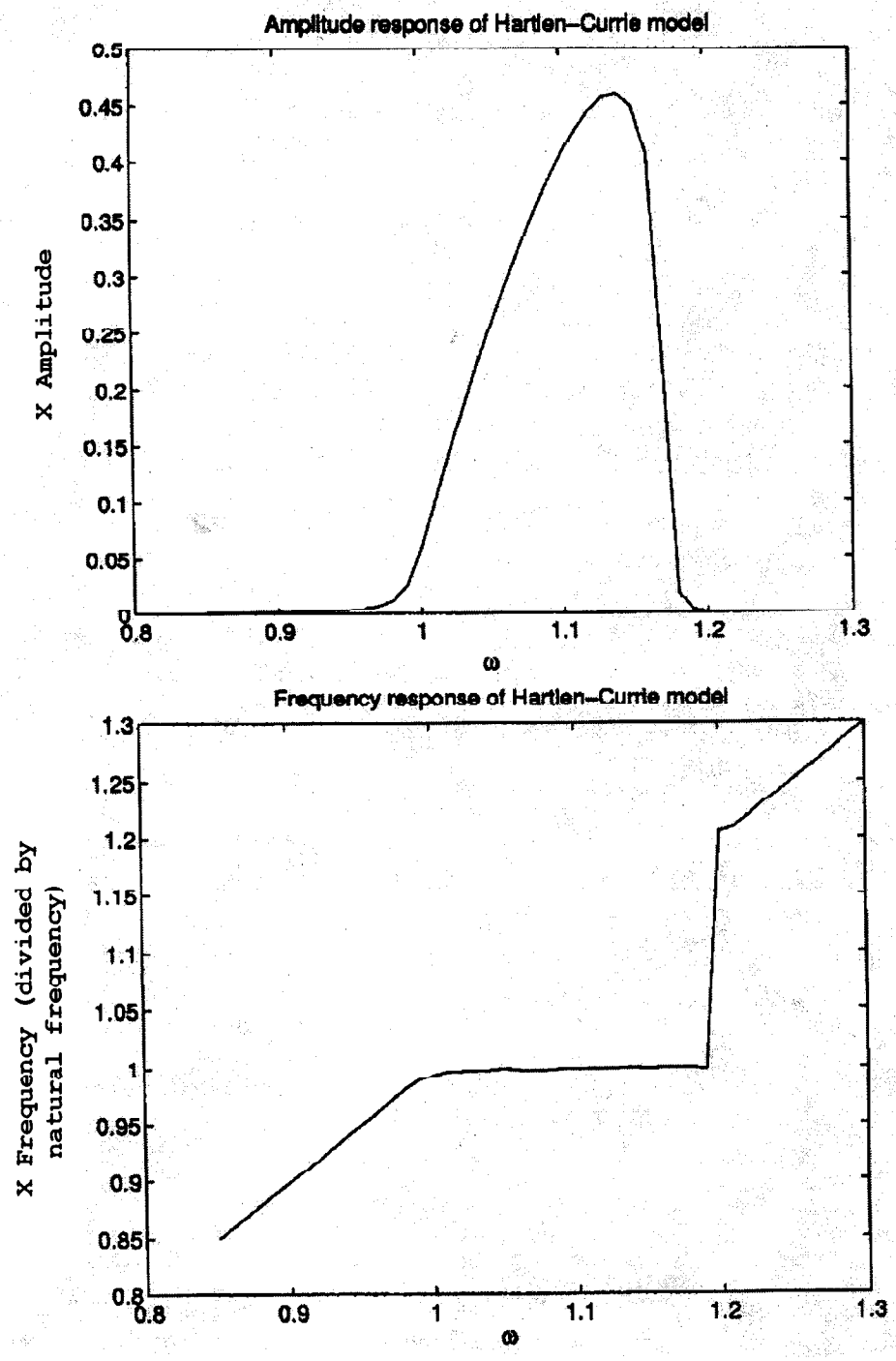

Figure 4. Numerical Integration of Hartlen and Currie Model (Note that model exhibits some of the features present in experimental data in figures 2 and 3.)

Various methods have been used to analyze the dynamics of wake oscillator models. Poore and Al-Rawi[9] have studied the Hartlen and Currie model in terms of Hopf bifurcations. Langford and Zhan[10] performed a more detailed study on a similar wake oscillator model also using the Hopf bifurcation theory. Corless and Parkinson[11, 12] have studied the Hartlen and Currie model using multiple scales perturbation techniques around the lock-in region. Using a variety of methods, Berger [13, 14] has studied a similar model with an additional cubic damping term in equation (2) and a cubic x coupling term in equation (3).

Figure 5 is an illustration of the amplitude and frequency response obtained from analysis of the Hartlen and Currie model using the original parameter values of equation (4). Features have been intentionally exaggerated to make them more visible. Arrows show jumps in amplitude and frequency occurring in response to sweeps of parameter ω (proportional to flow velocity), resulting in hysteresis. These jumps occur because of changes in stability and associated bifurcations of periodic motions. Figure 5 was obtained by studying the Hartlen and Currie model using multiple scales analysis and bifurcation analysis of the resulting slow-flow equations; see the appendix for details.

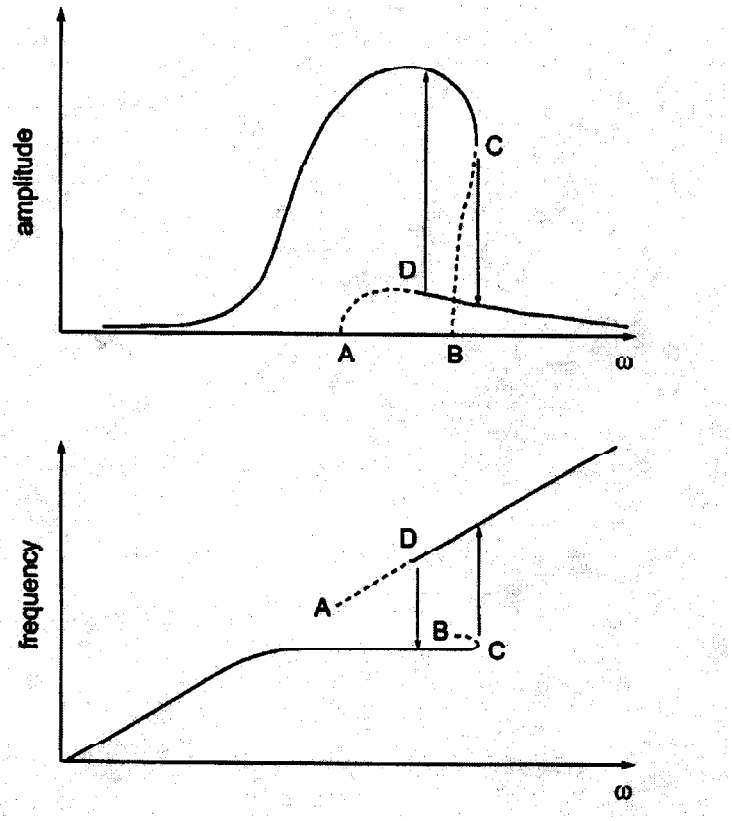

Figure 5. Amplitude and Frequency Response of Wake Oscillator Model (Horizontal axis ω is proportional to flow velocity. Vertical arrows represent jumps in response to slow sweeps in flow velocity and result in hysteresis. Solid lines represent stable branches of periodic motions, and dotted lines represent unstable branches.)

Corless[15] has studied the possible response diagrams for different parameter values in the Hartlen and Currie model. This analysis uses the multiple scales method and is restricted to small parameter values near the 1:1 resonance. The analysis also is restricted to examination of periodic motions and does not examine quasi-periodic motions or the possibility of chaos in the system.

CONCLUSIONS

As shown in this report, simplified models of vortex-induced vibrations have been extensively examined in the literature. Nevertheless, there are two areas in which further research is needed:

1. Although a great deal of attention has been paid to periodic motions, very little research has been focused on more complicated dynamical behaviors, such as quasi-periodic motions and chaos.

2. Recent experiments have shown that an important parameter affecting the qualitative behavior of vortex-induced vibrations is the ratio of cylinder mass to displaced fluid mass. Although wake oscillator models have successfully described experimental results for large mass ratios, little has been done to model systems with small mass ratios.

APPENDIX
RESULTS OF FREQUENCY AND AMPLITUDE RESPONSE

The results of the amplitude and frequency response obtained from analysis of the Hartlen and Currie model using the Hopf bifurcation theory and perturbation methods are complementary. The Hopf bifurcation theory gives approximations that are valid close to the origin; perturbation methods give approximations that are valid for small values of α, ζ, γ, a, b, and $\omega \approx 1$ (near the 1:1 resonance of the system). The results from perturbation methods allow the amplitude and frequency response of a system to be determined for a given set of parameter values. Analysis has shown that the dynamics of the system involve Hopf bifurcations from the origin where limit-cycle oscillations are created and destroyed. See Poore and Al-Rawi[9] for more on the Hopf bifurcation analysis.

In figure 5, points A and B correspond to Hopf bifurcations of the origin where limit cycles are created. Point C corresponds to a saddle-node bifurcation of cycles where the stability of the limit cycle changes along the branch. Point D corresponds to a torus bifurcation where a quasi-periodic motion is created. In the slow flow at point D, a subcritical Hopf bifurcation occurs where an unstable limit cycle (quasi-periodic motion in original equation) is created as ω increases and the stability of the equilibria (limit cycle in original equation) changes. Note that between points C and D there are two possible stable solutions. The arrows show the jumps in a hysteretic loop for increasing and decreasing flow speed (represented by ω). For a more detailed bifurcation analysis, see Guckenheimer and Holmes.[16]

A calculation similar to the one performed by Corless and Parkinson is presented below. To apply the method of multiple scales to the Hartlen and Currie model, a rescaling of equations (2) and (3) must first take place:

$$\alpha = \varepsilon, \quad 2\zeta = \varepsilon\beta, \quad a = \frac{\varepsilon^2 \hat{a}}{Y_0}, \quad b = Y_0 \hat{b}, \quad \gamma = \frac{4\alpha}{3Y_0{}^2},$$

and

$$y = Y_0 \hat{y}, \quad x = \varepsilon \hat{x} \quad \omega^2 = 1 + \varepsilon\delta, \tag{A-1}$$

where ε is considered a small perturbation parameter and δ is a measure of detuning off the 1:1 resonance. Substituting equations (A-1) into equations (2) and (3) and dropping the hats on terms gives

$$\ddot{x} + x = \varepsilon\left(-\beta\dot{x} + ay\right) + O\left(\varepsilon^2\right), \tag{A-2}$$

and

$$\ddot{y} + y = \varepsilon\left(-\delta y + \dot{y}\left(1 - \frac{4}{3}\dot{y}^2\right) + b\dot{x}\right) + O\left(\varepsilon^2\right). \tag{A-3}$$

Applying the method of multiple scales to equations (A-2) and (A-3) gives the following slow-flow equations:

$$\frac{dR_x}{d\eta} = -\frac{aR_y \sin(\varphi)}{2} - \frac{\beta R_x}{2}, \tag{A-4}$$

$$\frac{dR_y}{d\eta} = -\frac{R_y^3}{2} + \frac{R_y}{2} + \frac{bR_x \cos(\varphi)}{2}, \tag{A-5}$$

and

$$\frac{d\varphi}{d\eta} = -\frac{aR_y \cos(\varphi)}{2R_x} - \frac{bR_x \sin(\varphi)}{2R_y} - \frac{\delta}{2}, \tag{A-6}$$

where $x \approx R_x \cos(\xi - \theta_x)$, $y \approx R_y \cos(\xi - \theta_y)$, $\varphi = \theta_y - \theta_x$, $\xi = \omega t$, and $\eta = \varepsilon t$.

For more on the method of multiple scales, see Nayfeh and Mook[17] and Rand and Armbruster.[18] Equilibria in the slow flow correspond to periodic motions of the original system. Equations (A-4) – (A-6) can be combined to produce a single polynomial in R_x and the parameters a, b, β, and δ. The right-hand sides of equations (A-4) and (A-5) are set to zero, and then solved for $\sin\varphi$ and $\cos\varphi$. These expressions for $\sin\varphi$ and $\cos\varphi$ are then substituted back into the right-hand side of equation (A-6) and $\sin^2\varphi + \cos^2\varphi = 1$, producing two equations each involving R_x, R_y and the parameters a, b, β, and δ. These two equations can then be combined, eliminating R_y to give the following polynomial:

$$K_6 R_x^6 + K_4 R_x^4 + K_2 R_x^2 + K_0 = 0, \tag{A-7}$$

where

$$K_6 = b^2\beta^3,$$

$$K_4 = ab\beta^2(4\beta\delta - 2\delta - 3ab),$$

$$K_2 = a^2(\beta\delta^4 - ab\delta^3 + 2\beta^3\delta^2 - 2\beta^2\delta^2 + \beta\delta^2 - 5ab\beta^2\delta + ab\beta\delta + \beta^5 - 2\beta^4 + \beta^3 + 3a^2b^2\beta),$$

and

$$K_0 = -a^4(\beta\delta^2 - ab\beta\delta - ab\delta + \beta^3 - 2\beta^2 + \beta + a^2b^2).$$

Equation (A-7) produces the curves of the amplitude plot in figure 5. Determining the stability of the curves involves linearizing equations (A-4) – (A-6) around the equilibria and examining the eigenvalues of the system. The saddle-node bifurcation at point *C* occurs when an equilibrium point has a zero eigenvalue. The Hopf bifurcation at point *D* occurs when an equilibrium point has a pair of pure imaginary eigenvalues. These calculations are straightforward but result in lengthy expressions that have been omitted. In a similar fashion, a polynomial for the lock-in frequency can also be calculated, producing the second plot in figure 5.

REFERENCES

1. Private communication with T. Wei, Mechanical and Aerospace Engineering Department, Rutgers University, Piscataway, NJ, June 2000.

2. C. C. Feng, "The Measurement of Vortex-Induced Effects in Flow Past Oscillating and Stationary Circular and D-Section Cylinders," Master's Thesis, University of British Columbia, Vancouver, 1968.

3. R. Govardhan and C. H. K. Williamson, "Modes of Vortex Formation and Frequency Response of a Freely Vibrating Cylinder," *Journal of Fluid Mechanics*, vol. 420, 2000, pp. 85-130.

4. A. Khalak and C. H. K Williamson, "Motions, Forces and Mode Transitions in Vortex-Induced Vibrations at Low-Mass-Damping," *Journal of Fluids and Structures*, vol. 13, 1999, pp. 813-851.

5. R. D. Blevins, *Flow-Induced Vibrations, Second Edition*, Van Nostrand Reinhold, New York, 1990.

6. G. V. Parkinson, "Phenomena and Modelling of Flow-Induced Vibrations of Bluff Bodies," *Progress in Aerospace Science*, vol. 26, 1989, pp. 169-224.

7. R. E. D. Bishop and A. Y. Hassan, "The Lift and Drag Forces on a Circular Cylinder Oscillating in a Flow Field," *Proceedings of the Royal Society*, series A, vol. 277, 1964, pp. 32-75.

8. R. T. Hartlen and I. G. Currie, "Lift Oscillator Model for Vortex-Induced Vibrations," *American Society of Civil Engineers Journal of Engineering Mechanics*, vol. 96, 1970, pp. 577-591.

9. A. B. Poore and A. R. Al-Rawi, "The Dynamical Behaviour of the Hartlen-Currie Wake Oscillator Model," *Proceedings of the 5th International Conference on Wind Engineering*, 1979, pp. 1073-1083.

10. W. F. Langford and K. Zhan, "Dynamics of Strong 1:1 Resonance in Vortex-Induced Vibration," *Proceedings of ASME Symposium on Flow-Induced Vibration and Noise*, vol. 7, 1992, pp. 117-127.

11. R. M. Corless and G. V. Parkinson, "A Model of the Combined Effects of Vortex-Induced Vibration and Galloping," *Journal of Fluids and Structures*, vol. 2, 1988, pp. 203-220.

12. R. M. Corless and G. V. Parkinson, "A Model of the Combined Effects of Vortex-Induced Vibration and Galloping, Part II," *Journal of Fluids and Structures*, vol. 7, 1993, pp. 825-848.

13. E. Berger, "On a Mechanism of Vortex-Excited Oscillations of a Cylinder," *Journal of Wind Engineering and Industrial Aerodynamics*, vol. 28, 1988, pp. 301-310.

14. E. Berger and P. Plaschko, "Hopf Bifurcations and Hysteresis in Flow-Induced Vibration of Cylinders," *Journal of Fluids and Structures*, vol. 7, 1993, pp. 849-866.

15. R. M. Corless, "Bifurcations in a Flow-Induced Vibration Model," *Fields Institute Communications*, vol. 4, 1995, pp. 43-59.

16. J. Guckenheimer and P. Holmes, *Nonlinear Oscillators, Dynamical Systems, and Bifurcations of Vector Fields*, Springer-Verlag, New York, 1983.

17. A. H. Nayfeh and D.T. Mook, *Nonlinear Oscillations*, Wiley, New York, 1979.

18. R.H. Rand and D. Armbruster, *Perturbation Methods, Bifurcation Theory and Computer Algebra*, Springer-Verlag, New York, 1987.